



η^1 -silolyl-FeCp(CO)₂ complexes. Is there a way to sila-ferrocene?



Csaba Fekete^a, Réka Mokrai^a, Petra Bombicz^b, László Nyulászi^a, Ilona Kovács^{a,*}

^a Department of Inorganic and Analytical Chemistry, Budapest University of Technology and Economics, Szt. Gellért tér 4, Budapest, H-1111, Hungary

^b Institute of Organic Chemistry, Research Centre for Natural Sciences, Hungarian Academy of Sciences, Magyar Tudósok körútja 2, Budapest, H-1117, Hungary

ARTICLE INFO

Article history:

Received 17 July 2015

Received in revised form

11 September 2015

Accepted 19 September 2015

Available online 9 October 2015

Keywords:

Iron complex

Silacyclopentadiene

X-ray structure

Bissilol

DFT calculations

ABSTRACT

The reaction of 1-chlorosilols (**12**, **13**) and K[Fe(CO)₂Cp] in THF yielded two new η^1 -silolyl-FeCp(CO)₂ complexes (**15**, **16**) in good yield. These complexes are the first covalent Fe–Si bonded silolyl complexes reported in the literature, which were structurally proven by single crystal X-ray diffraction and multinuclear NMR spectroscopy. By temperature dependent NMR spectroscopy a rotational barrier of 14.4 kcal/mol was revealed, in agreement with the calculated 14.9 kcal/mol barrier of the phenyl rotation. The attempted transformation of these complexes to the corresponding silaferrocene by CO elimination failed. DFT calculations revealed that the rather high stability of the Si–Fe comparing to the C–Fe bond might be responsible for the stability of the complexes.

© 2015 Published by Elsevier B.V.

1. Introduction

One of the milestones in organometallic chemistry is the synthesis of ferrocene by Kealy and Pauson in 1951 and the determination of its structure by Wilkinson and Woodward in 1952. These achievements opened up the way to the use of metallocenes in applied and material science from polymerization catalysis to UV fluorescent materials [1]. Nowadays several metallocenes are known in which not just the central iron atom is replaced by other transition metals but also the ligands are changed to heterocyclopentadienyl analogues containing other main group elements such as P, As or Sb [2].

Interestingly, the number of known metallocenes possessing silicon or germanium containing heterocycles is small (Scheme 1). The first heavy metallocene analogue **1** was synthesized by Tilley et al. reacting Cp*[RuCl₄] with in situ generated Li[Me₄C₄GeSi(-SiMe₃)₃] [3], and the ferrocene analogue **2** was also published 9 years later [4]. The synthesis and NMR characterization of the first metallocene containing a silolyl ring (**3**) has been reported in 1994 [5]. Sekiguchi et al. synthesized metallocenes containing trisila- (**4**) and disilagermacyclopentadienyl (**5**) units using the appropriate complex source ([Cp*⁺RuCl]₄ or Cp*⁺Fe(acac)) and the lithium salt of

the heterocyclopentadienyl analogue [6,7]. Hafnium (**6**, **7**) and zirconium (**8**) complexes with a bent sandwich structure were also reported (Scheme 2) [8].

While the synthesis of the possible silaferrocene precursors (**9–11**) was also carried out, their transformation (by heating or UV irradiation) to the metallocenes was unsuccessful [9–11] (Scheme 3).

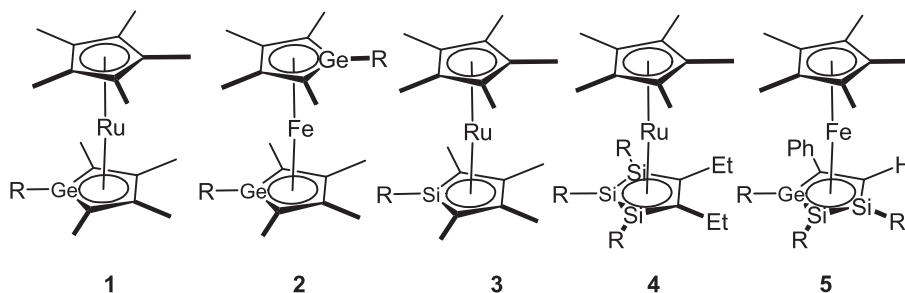
Recently, we studied the substituent effect on the aromaticity of the silolide anions, and reported that Me₃Si-substituents on the 2,5 position of the silolyl ring increase the aromaticity of the heterocycle significantly according to NICS and ISE_c values [12]. Since the stability of the ferrocene might be related to the aromaticity of the cyclopentadienyl moiety, we envisaged that using 2,5-trimethylsilyl-substituted silolyls the corresponding ferrocene analogues might be synthesized. Hereby, we report on two new η^1 -silolyl-FeCp(CO)₂ complexes, and their attempted transformation to the metallocenes, completed with DFT calculations for a better understanding of the experimental results.

2. Results and discussion

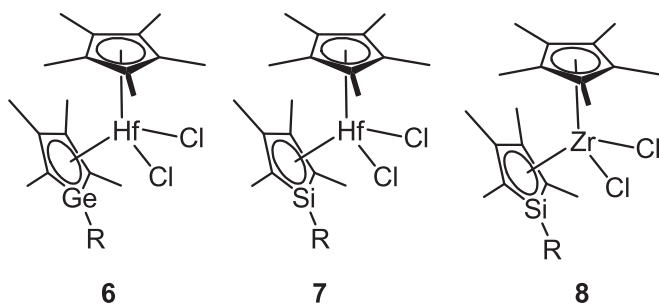
We reported recently the synthesis of **12**, via an amine – chloride exchange route developed originally by Tamao [13,14]. The synthesis of **13** was performed in an analogous manner, using Et₂NSiMeCl₂ as starting material. **14** was synthesized by the reaction between **12** and *t*BuLi in THF at –50 °C. Interestingly the ¹H and

* Corresponding author.

E-mail address: ikovacs@mail.bme.hu (I. Kovács).



Scheme 1. Metallocenes containing group 14 metallols.



Scheme 2. Bent sandwich complexes.

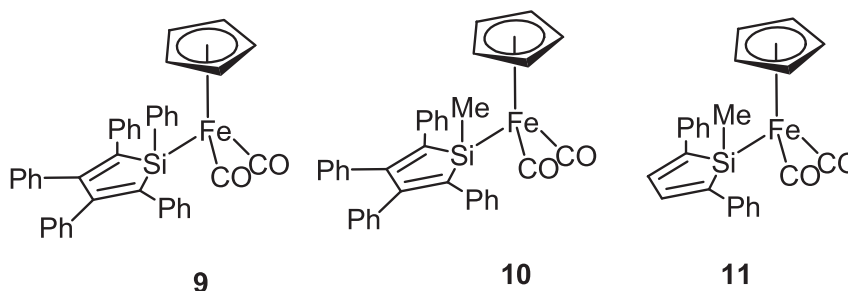
^{13}C NMR spectra of **13** and **14** show that the signals connected to the ortho- and meta-hydrogens and carbons of the phenyl groups on the β carbons of the silolyl ring show splitting or become broad at room temperature indicating a restricted rotation of the phenyl moiety. From temperature dependent ^{13}C and ^1H NMR measurements (temperature range 233–333 K, solvent CDCl_3) a coalescence temperature $T_c = 313$ K was determined for **14** (F. S1), allowing to calculate a rotational barrier of $\Delta G_{\text{rot}} = 14.4$ kcal/mol. This value is in excellent agreement with the DFT calculated phenyl rotation barrier ($\Delta G_{\text{rot}} = 14.9$ kcal/mol B3LYP/6-311 + G*). The optimized transition structure of the phenyl rotation is shown in Fig. S2.

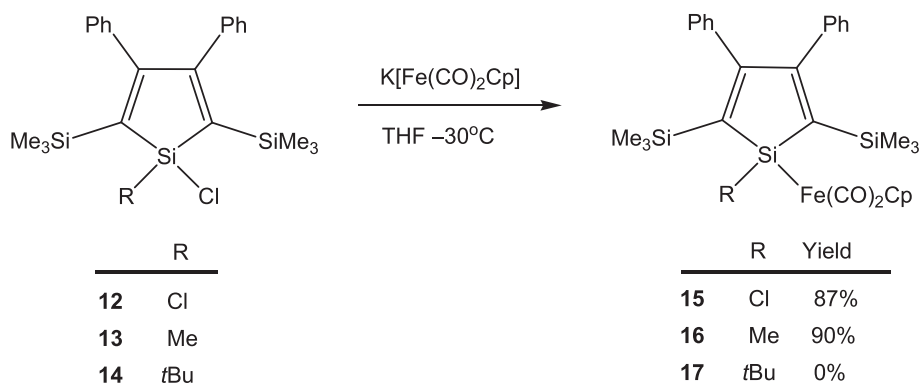
While 1-chlorosilols (**12**, **13**) provided complexes **15**, **16** in good yield when reacted with $\text{K}[\text{Fe}(\text{CO})_2\text{Cp}]$ in THF at -30°C , **14** failed to give the expected **17** even when the mixture was heated to reflux temperature, probably due to the steric hindrance of the bulky *t*Bu-substituent on the silicon (Scheme 4). Likewise, the attempted reactions with $\text{K}[\text{W}(\text{CO})_3\text{Cp}]$ aiming to form a tungsten complex failed even in THF at reflux temperature. Complexes **15** and **16** were identified by ^1H , ^{13}C , and ^{29}Si NMR. The ring ^{29}Si NMR chemical shift of **15** ($\delta = 82.6$ ppm) is in the same region as that of $\text{CpFe}(\text{CO})_2\text{SiMe}_2\text{Cl}$ ($\delta = 86.36$ ppm) [15]. Similarly, the ^{29}Si NMR chemical shift of the ring silicon atom in **16** ($\delta = 55.5$ ppm) is close to the

reported chemical shift of **10** ($\delta = 47.59$ ppm) [10]. This behaviour indicates that while the variation of the substituents directly at silicon has a significant impact on the chemical shielding, changes at the α carbon atoms have only a small influence on the ^{29}Si NMR chemical shift values of the Si atom in the five membered ring. ^{13}C NMR chemical shifts of complex **15** and **16** indicated similar restricted rotation of the phenyl groups as mentioned before in the case of **13** and **14**. The ^{13}C NMR chemical shift of the Cp carbons in **15** ($\delta = 85.2$ ppm) and **16** ($\delta = 85.1$ ppm) is somewhat downfielded with respect to **10** ($\delta = 84.2$ ppm) [10]. IR bands of the carbonyl groups of **15** and **16** (**15**: 2011, 1957 cm^{-1} ; **16**: 1999, 1948 cm^{-1}) were measured in nujol film and are in the region of the previously synthesized η^1 -silolyl- $\text{FeCp}(\text{CO})_2$ complexes (Scheme 3: **9**: 2010, 1960 cm^{-1} in CH_2Cl_2 ; **10**: 1995, 1943 cm^{-1} in benzene; **11**: 2015, 1955 cm^{-1} in cyclohexane [9–11]).

Recrystallization of **15** and **16** from hexane at -30°C resulted in single crystals suitable for X-ray diffraction study; the structures are shown in Figs. 1 and 2.

15 and **16** crystallizes in the monoclinic crystal system $P2_1/c$ and $P2_1/n$, respectively. Crystal data and details of the structure determination and refinement are listed in Tables S3–S13. There is one molecule in the asymmetric unit, and no molecular symmetry could be found in the compounds. The molecular conformation around the Fe centre is presented in Table S5. The silolyl rings are slightly twisted [16] on Si1 (0.0732(14) Å) and C8 (−0.081(3)) in **15** and on Si1 (−0.0590(9) Å) and C5 (0.0553(19)) in **16**. Typical bond lengths and endocyclic bond angles can be found in the silolyl rings of **15** and **16** (Table S6) [17]. The silicon centre has distorted tetrahedral geometry (Table S7). The endocyclic C–Si–C angles are $94.40(13)^\circ$ in **15** and $93.10(8)^\circ$ in **16** due to the constraints imposed by the five member ring, while in spite of the chemical difference the Cl1–Si1–Fe1 angle ($112.86(4)^\circ$) in **15** is very close to the C1–Si1–Fe1 angle ($112.67(6)^\circ$) in **16**. The molecular conformations are stabilized by C–H ... π intramolecular interactions between the Me_3Si group and the neighbouring phenyl ring. The Cp C–H gets close to the silolyl ring in **16** (2.53 Å), while it does not happen in **15**

Scheme 3. η^1 -silolyl- $\text{FeCp}(\text{CO})_2$ complexes.



Scheme 4. Synthesis of η^1 -silolyl-FeCp(CO)₂ complexes **15** and **16**.

because the Cp moiety turns with an edge of the pentagon to the silolyl ring. There is no $\pi \dots \pi$ interaction in **15**, while intermolecular $\pi \dots \pi$ interaction is found between the Cp rings in the crystal lattice of **16** with the distance of 3.8862(14) Å.

Further comparing the structural features of **15** and **16** it is noteworthy that the Fe–Si bond is longer by 0.0597(9) Å in **16** than in **15**, indicating that the presence of chlorine substituent at Si strengthens the Fe–Si bond. Clearly, the doubly filled Fe d orbital(s) interact in a negative hyperconjugation with the σ^* orbital at Si, and the interaction is much stronger in the SiCl than in the SiMe case based on NBOdel calculations on model systems (See Supplementary information S2) [18]. This negative hyperconjugative effect was already assumed in the case of CpFe(CO)₂SiCl₃ where the Fe–Si bond length was shorter than expected from the covalent radii ($d(\text{Fe}–\text{Si}) = 2.21$ Å) [19]. In accordance the π -donor ability of the central Fe in **15** is smaller than in **16**, resulting in a reduction of the π -back bonding. This strengthens the CO bond of the carbonyl ligands, as indicated by the increasing wavenumber of the CO stretching frequency as was already noted above. Also the tendency of slight increase of the Fe–C bond length in **15** compared to **16** confirms this explanation ($d(\text{Fe}–\text{CO}) =$ **15**: 1.744(3), 1.755(3) Å **16**:

1.7425(19), 1.750(2) Å). Our results also agree with the known σ -donor behaviour of Si in Fe–Si bond [20].

The attempt to transform **15** and **16** to the desired silaferrocene was carried out similar way as published in the case of the carbon analogue [21]. Refluxing the toluene solution of **15** and **16** did not result in any change even after 1 week. UV irradiation of **16** using a high-pressure mercury lamp in a hexane solution did not result again in the desired silaferrocene, however, the dimeric iron complex ([FeCp(CO)₂]₂) and bissilol (**18**) has been formed in low yield. Interestingly a similar reaction occurred during the irradiation of the mixture of FpSiPh₃ and FpMe (Fp = CpFe(CO)₂) yielding MeSiPh₃ and [FeCp(CO)₂]₂, however in this reaction no disilane formation was detected [15]. In the case of **15** the decomposition of the silolyl ring was observed during the irradiation (likewise, decomposition was reported in case of **11** [11]). The different behaviour of **15** and **16** (Scheme 5) might be related to the above discussed increased stability of the Si–Fe bond in case of **15** blocking the decomposition pathway, which leads to the formation of the radicals yielding easily the dimeric products. Interestingly during the MS measurements of the methyl-derivate (**16**) the silolyl fragment [Ph₂(SiMe₃)₂C₄SiMe]⁺ was detected as the base peak,

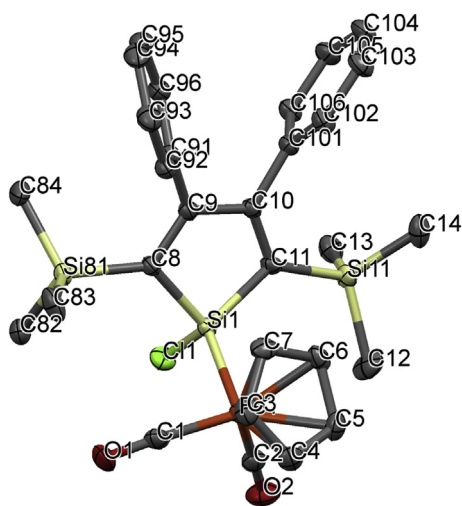


Fig. 1. ORTEP diagram of **15** at 50% probability level (hydrogen atoms are omitted for clarity). Selected bond lengths (Å) and angles (°): Fe(1)–Si(1) 2.3064(8), Si(1)–Cl(1) 2.1043(10), Fe(1)–C(1) 1.755(3), Fe(1)–C(2) 1.745(3), C(1)–O(1) 1.148(4), C(2)–O(2) 1.164(4), Si(1)–C(8) 1.886(3), Si(1)–C(11) 1.883(3), C(8)–C(9) 1.362(4), C(9)–C(10) 1.516(4), C(10)–C(11) 1.359(4); C(11)–Si(1)–C(8) 94.40(12), C(11)–Si(1)–Cl(1) 106.86(9), C(8)–Si(1)–Cl(1) 108.84(9), C(11)–Si(1)–Fe(1) 117.46(9), C(8)–Si(1)–Fe(1) 114.73(9), Cl(1)–Si(1)–Fe(1) 112.85(4).

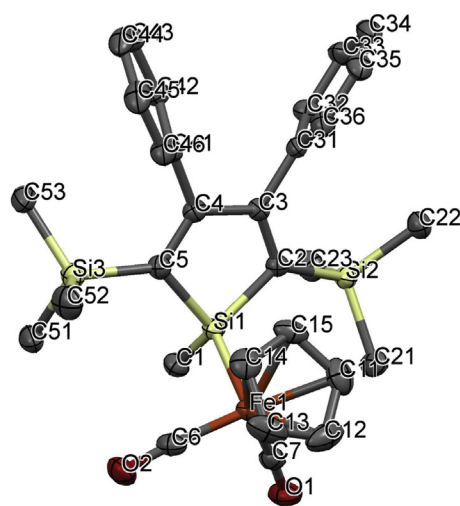
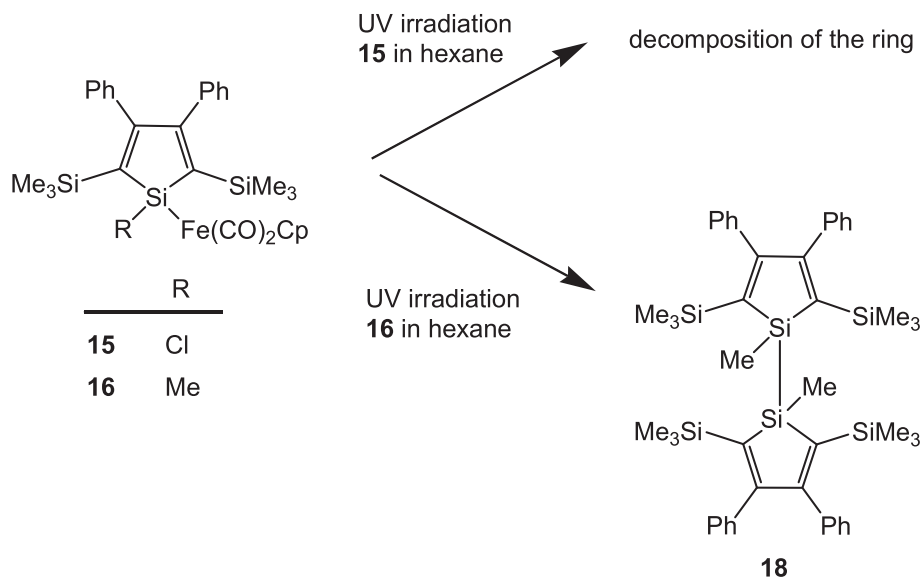


Fig. 2. ORTEP diagram of **16** at 50% probability level (hydrogen atoms are omitted for clarity). Selected bond lengths (Å) and angles (°): Fe(1)–Si(1) 2.3660(5), Si(1)–C(1) 1.8815(18), Fe(1)–C(6) 1.742(2), Fe(1)–C(7) 1.750(2), C(6)–O(2) 1.161(2), C(7)–O(1) 1.154(2), Si(1)–C(2) 1.9022(18), Si(1)–C(5) 1.8945(18), C(2)–C(3) 1.359(2), C(3)–C(4) 1.512(2), C(4)–C(5) 1.363(2); C(5)–Si(1)–C(2) 93.10(8), C(1)–Si(1)–C(5) 113.74(8), C(1)–Si(1)–C(2) 110.44(8), C(1)–Si(1)–Fe(1) 112.67(6), C(5)–Si(1)–Fe(1) 110.84(6), C(2)–Si(1)–Fe(1) 114.66(6).

Scheme 5. UV Irradiation of **15** and **16**.

which might be related to the cleavage of the Fe–Si bond, while in case of **15** there was no sign of a similar fragmentation route.

We succeeded in growing a single crystal from **18**, allowing its structural characterization (Fig. 3). **18** crystallizes in the triclinic crystal system, the space group is *P*-1. In the lack of strong secondary interactions in the crystal lattice of **18** the crystal quality

was low. Crystal data and details of the structure determination and refinement are listed in Tables S3–S13. There is one molecule in the asymmetric unit. The planar silolyl rings have the angle of 52.64(14)° (Table S4). A trimethylsilyl C–H gets close to the silolyl ring in **18** with the distance of 2.85 Å contributing to the stability of the curved shape of the molecule. The structural features are similar to the other silols. Comparing the Si–C_α, C_α–C_β and C_β–C_β bond length of the silolyl ring in bis-silol **18** with those of **16** revealed that these bond lengths change only slightly when the iron centre is connected to the Si. The relatively long C_β–C_β bonds in the complexes **15**, **16** and in **18** can be attributed to the repulsion of the neighbouring phenyl groups in the β position. We have shown the effectiveness of this interaction in case of the silolid dianion [13]. The other effect which might be responsible for the increased C_β–C_β bond length in silols compared to phosphole is that the C_α–Si–C_α angle about the tetrahedral silicon (109.47°) is much wider than the near 90° bonding angle about phosphorus [22], which results in an apparent increase of the C_β–C_β distance (Fig. 3, C(3)–C(4) and C(7)–C(8)). It is noteworthy that the Si–Si bond in **18** (2.4632(13) Å) is longer than the previously reported for 1,1-bissilols (2.354(3)–2.375(1) Å) [23], apparently due to the bulky trimethylsilyl-substituents at the C_α carbons. (e.g. Si–Si distance is 2.433(1) Å in *t*Bu₂HSi–SiH*t*Bu₂ [24], and 2.697(3) Å in *t*Bu₃Si–Si*t*Bu₃ [25]).

In a further attempt to get silaferrocenes complexes, **15** and **16** were treated with Me₃NO to eliminate CO groups from the complex but no reaction took place even after stirring the mixture for 3 days in THF solution at reflux temperature [26]. After all attempts to eliminate the CO ligands from the complexes **15** and **16** were unsuccessful, DFT calculations were carried out to understand the observed stability of the η¹-complexes.

3. Calculations

The energy and Gibbs free energy values (at 293 K, atmospheric pressure) of the decomposition of the η¹-complexes to metallocenes are given for model compounds in Table 1.

In the case of the carbon analogue the energy difference between the starting material and the products is positive, but the Gibbs free energy difference (at 298 K and atmospheric pressure) is negative due to the formation of two free carbon-monoxid

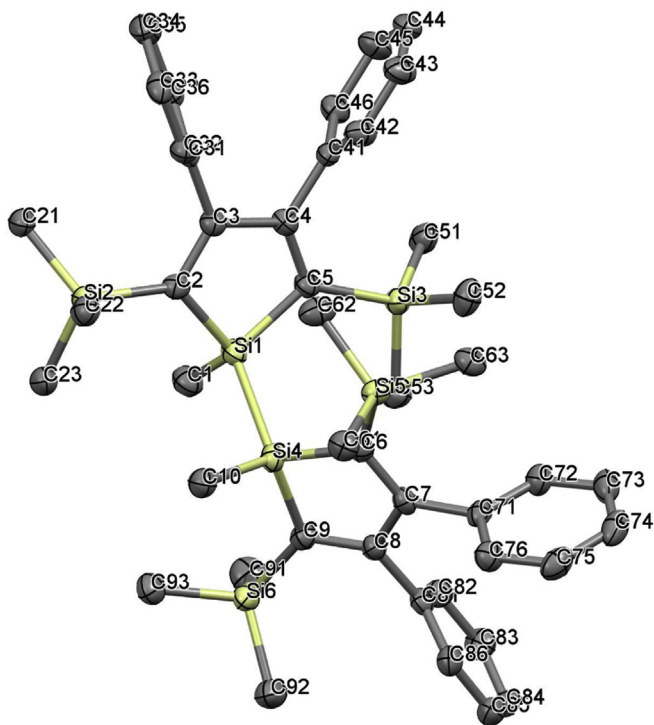
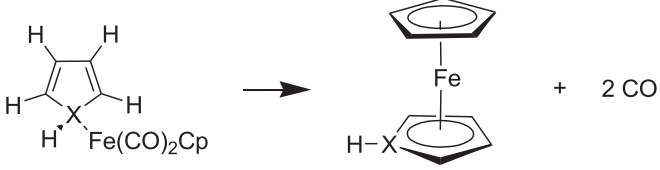


Fig. 3. ORTEP diagram of **18** at 50% probability level (hydrogen atoms are omitted for clarity). Selected bond lengths (Å) and angles (°): Si(1)–Si(4) 2.4632(12), Si(1)–C(2) 1.891(3), Si(1)–C(1) 1.881(3), Si(1)–C(5) 1.886(3), C(2)–C(3) 1.369(4), C(3)–C(4) 1.519(4), C(4)–C(5) 1.359(4), Si(4)–C(10) 1.870(3), Si(4)–C(6) 1.878(3), Si(4)–C(9) 1.885(3), C(6)–C(7) 1.363(4), C(7)–C(8) 1.511(4), C(8)–C(9) 1.366(4); C(1)–Si(1)–C(5) 110.65(14), C(1)–Si(1)–C(2) 111.06(14), C(5)–Si(1)–C(2) 94.40(13), C(1)–Si(1)–Si(4) 110.46(11), C(5)–Si(1)–Si(4) 115.15(10), C(2)–Si(1)–Si(4) 114.23(10).

Table 1
B3LYP/6-311 + G* energy and Gibbs free energy values (in kcal/mol) for CO elimination reactions.



X	ΔE	ΔG
C	7.3	-15.7
Si	44.8	21.1
Ge	43.6	20.3

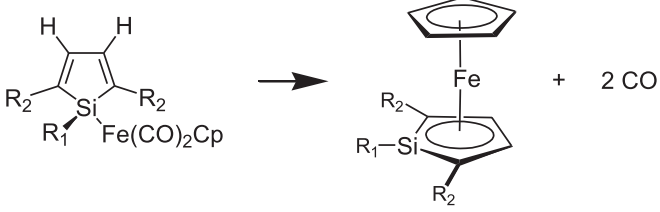
molecules, in agreement with the result of Yates and co-workers [27]. The stability of the η^1 -complex is much larger in case of the silolyl (and also for the germolyl) rings and accordingly even the Gibbs free energy difference remains positive. The energy of the CO elimination reaction was also calculated for differently substituted silols but in no case was the ferrocene analogue significantly stabilized (Table 2).

Calculations on the model η^1 -complexes revealed that the Mulliken charge at Fe is getting somewhat more negative when replacing the cyclopentadienyl ligand by silolyl (1.69 and 1.62, respectively), despite the fact that the electronegativity of silicon is smaller than that of carbon. Also the s character of the Si (28%) in the Si–Fe bond is significantly larger than the s character of C (19%) in the C–Fe bond based on NBO calculations. It is noteworthy that a comparative Mössbauer spectral study on $\text{CpFe}(\text{CO})_2\text{SiMe}_3$ and $\text{CpFe}(\text{CO})_2\text{CH}_3$ provided similar results [20].

We also studied the energy difference between the isomers shown in Fig. 4. It was revealed that the most stable isomer is (by about 40 kcal/mol) where iron is connected to silicon. The stabilization can partly be attributed to the stability of the $\text{Fe}^{(+)}\text{–Si}$ bond energy, which is apparently rather stable in comparison with the $\text{Fe}^{(+)}\text{–C}$ bond as shown by the energy difference of the isomers $\text{Cp}(\text{CO})_2\text{FeSiH}_2\text{CH}_3$ and $\text{Cp}(\text{CO})_2\text{FeCH}_2\text{SiH}_3$ (Fig. 5), although the different Si–H and C–H bond energies also contribute to the relative stabilities.

A further stabilizing contribution comes from the ca. 30 kcal/mol stability difference of the C=C and Si=C double bonds [28], as shown by the energy difference of the constitution isomers of silol

Table 2
B3LYP/6-311 + G* energy and Gibbs free energy values (in kcal/mol) of the CO elimination reaction for different substituted silolyl-complexes.



R ₁	R ₂	ΔE	ΔG
Cl	H	49.5	25.3
Me	H	42.7	19.0
OMe	H	48.8	24.1
SiH ₃	H	41.2	17.6
H	Cl	51.4	25.3
H	OMe	56.6	31.0
H	SiH ₃	44.6	20.6

($\text{H}_2\text{SiC}_4\text{H}_4$) (Fig. 6). Clearly, the facile 1, 5 shift, resulting in a fluxional behaviour of η^1 -cyclopentadienyl- $\text{FeCp}(\text{CO})_2$ (and other cyclopentadienyl derivatives) is hindered in the case of the silolyl derivate [29]. The stability of structure A (Fig. 6) is especially noteworthy, since the Si–H bond is weaker than the C–H.

4. Conclusion

The synthesis of the new silols (**13**, **14**) and η^1 -silolyl- $\text{FeCp}(\text{CO})_2$ complexes (**15**, **16**) were carried out. **15** and **16** are the first Fe–Si covalent bonded silolyl complexes reported in the literature, which are characterized by ^1H , ^{13}C , and ^{29}Si NMR, IR spectroscopies, as well as with single crystal X-ray diffraction. Transformation of these complexes to a ferrocene analogue sandwich complexes were unsuccessful using UV irradiation, Me_3NO or by simple heating. The reason for the increased stability of these carbonyl complexes can be attributed to the increased σ -electron donating behaviour of the silicon to the central Fe, while the aromaticity of the silolyl ligand seems to have less influence. According to our experiences there is little chance to obtain sandwich complexes from decarbonylation η^1 -silolyl- $\text{FeCp}(\text{CO})_2$ complexes.

5. Experimental section

5.1. General

All reactions were performed in oven-dried glassware under dried nitrogen or argon using standard Schlenk techniques. Solvents were dried according to well-known procedures (THF, diethyl ether, dioxane, and C_6D_6 over sodium/benzophenone, hexane over LiAlH_4) and distilled freshly before use. Solids were dried in vacuum. CDCl_3 was dried over activated molecular sieves. 1.6 M *n*-butyl lithium and 1.6 M *tert*-butyl lithium solution in hexane from Merck Ltd. were used directly. NMR spectra were recorded on a Bruker Avance 300 and a Bruker DRX-500 spectrometers (standard: external TMS, chemical shifts are given in ppm). HMBC, HMQC and DEPT measurements were carried out to interpret the signals of the phenyl and silolyl rings. Infrared spectra were recorded using Perkin Elmer System 2000 FT-IR spectrometer from 4000 to 400 cm^{-1} in nujol film. High-resolution mass spectra were recorded with a Varian MAT 8200 mass spectrometer. Irradiations with UV light were carried out using HPK-125W high-pressure mercury vapour lamp. Elemental analysis was performed with an Elemental vario EL analyser.

The single crystal of **15**, **16** and **18** were mounted on a loop. Intensity data were collected on a RAXIS-RAPID diffractometer (monochromator; Mo-K α radiation, $\lambda = 0.71073\text{ \AA}$) at 93(2) K. The structures were solved by direct methods [30] (and subsequent difference syntheses). Hydrogen atomic positions were calculated from assumed geometries. Hydrogen atoms were included in structure factor calculations but they were not refined. The isotropic displacement parameters of the hydrogen atoms were approximated from the $U(\text{eq})$ value of the atom they were bonded to. The molecular graphics were prepared using the software Mercury [31].

5.2. Calculations

Geometry optimizations and energy calculations for complexes were carried out at the B3LYP/6-311 + G* level with Gaussian09 package [32], followed by calculation of the second derivatives to ensure that real minima were obtained (Tables 1 and 2). For larger systems such as complex **15** and **16** generated basis set (supplementary information S9) were applied for B3LYP method. On the silolyl ring (SiC_4) and the $\text{Fe}(\text{CO})_2\text{Cp}$ fragment 6-311 + G*, while on

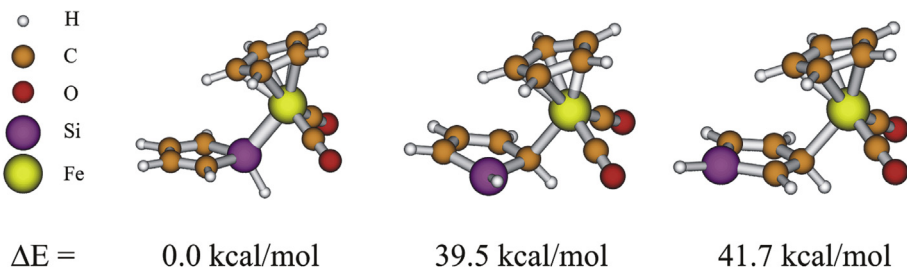


Fig. 4. Energy differences of the calculated structures of the different constitution isomers of $\text{CpFe}(\text{CO})_2\text{SiC}_4\text{H}_5$.

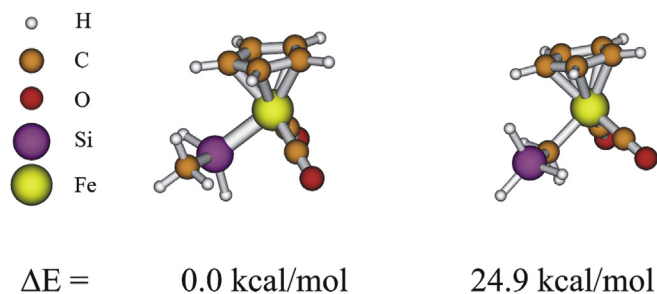


Fig. 5. Energy difference of the calculated structures of the $\text{Cp}(\text{CO})_2\text{FeSiH}_2\text{CH}_3$ and $\text{Cp}(\text{CO})_2\text{FeCH}_2\text{SiH}_3$.

the substituents of the silolyl ring (phenyl rings on C_2 carbons and trimethylsilyl-groups on C_1 carbons) 6-31 + G^* method were used. NBO calculations were carried out on the optimized geometries [33]. Tables with the calculated geometries are given in the Supplementary materials. For the visualization of the structures the Molden program was used [34].

5.3. 1,1-Dichloro-3,4-diphenyl-2,5-bis(trimethylsilyl)-1-silacyclopentadiene (**12**)

The synthesis was carried out according to Tamao's procedure [13,14]. The ^1H , ^{13}C , and ^{29}Si NMR data of the product were in agreement with the previously reported results. M.p. 78–81 °C. ^1H NMR (CDCl_3): $\delta = 0.22$ (s, r 18H, SiMe_3), 6.67–6.96 (m, 10H, ArH). ^{13}C { ^1H } NMR (CDCl_3): $\delta = 0.3$ (SiMe_3), 127.0 (*pPh*), 127.5, 128.4 (*o/mPh*), 136.2 (C_α), 140.4 (*iPh*), 169.8 (C_β). ^{29}Si { ^1H } NMR (C_6D_6): $\delta = 19.3$ (Si-ring), –7.9 (SiMe_3).

5.4. 1-Chloro-1-methyl-3,4-diphenyl-2,5-bis(trimethylsilyl)-1-silacyclopentadiene (**13**)

Synthesis was carried out by a similar way as Tamao's route [13,14] using $\text{MeSi}(\text{NEt}_2)\text{Cl}_2$ as starting material instead of $\text{Si}(\text{NEt}_2)_2\text{Cl}_2$. 0.606 g (86.6 mmol) lithium was added to a THF (200 mL) solution of 11.25 g (86.6 mmol) naphthalene and the

mixture was stirred under argon atmosphere at room temperature for 4 h. The mixture was cooled to –78 °C and 6.86 g (21.6 mmol) diethylamino-methyl-bis(phenylethynyl)silane were added dropwise to it, and was stirred for 1 h at the same temperature. The mixture was quenched with 10.33 g (95.2 mmol) trimethylchlorosilane at –78 °C, allowed to warm to room temperature and condensed under reduced pressure. After the addition of dry hexane the insoluble lithium-chloride were filtered and the solvent was condensed under reduced pressure, followed by the removal of the naphthalene by sublimation (at 100 °C/0.1 mbar). The residue was dissolved in 130 mL diethyl ether and dry HCl gas generated from NH_4Cl (11.58 g, 0.216 mmol) and H_2SO_4 (11.5 mL, 0.216 mol) was bubbled through it at –78 °C over 2 h. The mixture was allowed to warm to room temperature, and was condensed under reduced pressure. After the addition of dry hexane the insoluble salts were filtered and filtrate was condensed under reduced pressure. **13** was obtained by distillation at reduced pressure (160–180 °C/0.01 mbar) and was purified by recrystallization from hexane solution at –30 °C, yielded 6.02 g (65%) colourless crystals. M.p. 97–98 °C. Anal. Calcd. for $\text{C}_{23}\text{H}_{31}\text{ClSi}_3$ (427.21): C, 64.66; H, 7.31. Found: C, 63.96; H, 7.64. ^1H NMR (CDCl_3): $\delta = -0.06$ (s, 18H, SiMe_3), 0.82 (s, 3H, Me), 6.7–7.1 (m, 10H, ArH). ^{13}C { ^1H } NMR (CDCl_3): $\delta = 0.4$ (SiMe_3), 0.9 (SiCH_3), 126.6 (*pPh*), 127.0 (*o/mPh*), 128.4 (*o/mPh*), 139.7 (C_α), 141.4 (*iPh*), 169.7 (C_β). ^{29}Si { ^1H } NMR (C_6D_6): $\delta = 30.4$ (Si-ring), –8.7 (SiMe_3). HRMS (EI): m/z (%) 426.1412 (calc. for $\text{C}_{23}\text{H}_{31}\text{ClSi}_3$ 426.1417) (45.8), 428.1377 (calc. for $\text{C}_{23}\text{H}_{31}\text{ClSi}_3$ 428.1387) (21.5) [M^+], 411.1177 (calc. for $\text{C}_{22}\text{H}_{28}\text{ClSi}_3$ 411.1187) (33.4), 413.1142 (calc. for $\text{C}_{22}\text{H}_{28}\text{ClSi}_3$ 413.1158) (15.4) [$\text{M}^+ - \text{Me}$].

5.5. 1-Chloro-1-tert-butyl-3,4-diphenyl-2,5-bis(trimethylsilyl)-1-silacyclopentadiene (**14**)

3.97 g (8.88 mmol) **12** was dissolved in 80 mL THF and cooled to –50 °C and *t*BuLi (1.51 M in hexane, 5.9 mL, 8.88 mmol) was added dropwise to this solution. The resulting brownish green mixture was stirred for another 1 h at the same temperature. After that the reaction mixture was allowed to warm to room temperature and was stirred overnight. The solvents were removed at reduced pressure resulting in a red residue. After addition of 20 mL hexane the mixture was filtered, and the pure compound was

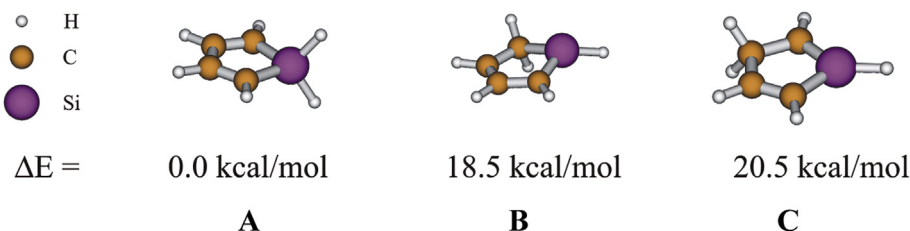


Fig. 6. Energy differences of the calculated structures of the different silols.

obtained by crystallization from hexane at $-30\text{ }^{\circ}\text{C}$, yielded: 2.70 g (65%). M.p. $120\text{--}122\text{ }^{\circ}\text{C}$. Anal. calcd. for $\text{C}_{26}\text{H}_{37}\text{Si}_3\text{Cl}$ (469.29): C, 66.54; H, 7.95%. Found: C, 66.23; H, 7.90. ^1H NMR (CDCl_3): $\delta = 0.10$ (s, 18H, SiMe₃), 1.24 (s, 9H, *t*Bu), 6.65–7.1 (m, 10H, ArH). $^{13}\text{C}\{^1\text{H}\}$ NMR (CDCl_3): $\delta = 1.2$ (SiMe₃), 21.4 (C(CH₃)₃), 27.7 (C(CH₃)₃), 126.6 (*p*Ph), 126.9, 127.0, 128.5, 129.4 (*o/m*Ph), 138.6 (C _{α}), 141.5 (*i*Ph), 171.6 (C _{β}). $^{29}\text{Si}\{^1\text{H}\}$ NMR (C_6D_6): $\delta = 33.9$ (Si-ring), -8.8 (SiMe₃) HRMS (EI): *m/z* (%) 468.1886 (calc. for $\text{C}_{26}\text{H}_{37}\text{Si}_3\text{Cl}$ 468.1892) (15.8), 470.1854 (calc. for $\text{C}_{26}\text{H}_{37}\text{Si}_3\text{Cl}$ 470.1862) (7.3) [M^+], 411.1169 (calc. for $\text{C}_{22}\text{H}_{28}\text{Si}_3\text{Cl}$ 411.1187) (22.8), 413.1140 (calc. for $\text{C}_{22}\text{H}_{28}\text{Si}_3\text{Cl}$ 413.1158) (13.7) [$\text{M}^+ - \text{tBu}$].

5.6. (1-Chloro-3,4-diphenyl-2,5-bis(trimethylsilyl)-1-silacyclopentadienyl)- η^5 -cyclopentadienyl-dicarbonyl-iron (**15**)

10 mL THF was added to 0.23 g (1.05 mmol) $\text{K}[\text{Fe}(\text{CO})_2\text{Cp}]$ and the resulting mixture was cooled to $-40\text{ }^{\circ}\text{C}$. During the dropwise addition of 0.47 g (1.05 mmol) **12** in 10 mL THF, the colour of the mixture first became orange and after the addition was completed it is turned to brown. The reaction mixture was stirred for an additional 15 min at $-40\text{ }^{\circ}\text{C}$ and was subsequently allowed to warm to room temperature and was stirred for another 2 h at the same temperature. The solvent was removed under reduced pressure and 15 mL hexane was added to the residue. The resulting insoluble white salt was filtered out and the brown filtrate was concentrated under reduced pressure and crystallized at $-30\text{ }^{\circ}\text{C}$ to get yellow needles. Yield: 0.45 g (73%). Anal. calcd. for $\text{C}_{29}\text{H}_{33}\text{Si}_3\text{FeO}_2\text{Cl}$ (589.12): C, 59.12; H, 5.65. Found: C, 58.82; H, 5.67. ^1H NMR (C_6D_6): $\delta = 0.19$ (s, 18H, SiMe₃), 4.28 (s, 5H, Cp), 6.7–7.0 (m, 10H, Ph). $^{13}\text{C}\{^1\text{H}\}$ NMR (CDCl_3): $\delta = 1.5$ (SiMe₃), 85.1 (Cp), 126.5 (*p*Ph), 127.2, 128.9, 129.8 (*o/m*Ph), 142.5 (C _{α}), 150.8 (*i*Ph), 162.0 (C _{β}), 213.9 (CO). $^{29}\text{Si}\{^1\text{H}\}$ NMR (CDCl_3): $\delta = 82.6$ (Si-ring), -8.7 (SiMe₃). IR (nujol, cm^{-1}) $\nu(\text{CO})$ 2011, 1957. HRMS (EI): *m/z* (%) 588.0828 (calc. for $\text{C}_{29}\text{H}_{33}\text{ClFeO}_2\text{Si}_3$ 588.0826) (76.3), 590.0836 (calc. for $\text{C}_{29}\text{H}_{33}\text{ClFeO}_2\text{Si}_3$ 590.0797) (17.7) [M^+], 532.0931 (calc. for $\text{C}_{27}\text{H}_{33}\text{ClFeSi}_3$ 532.0928) (4.1), 534.0920 (calc. for $\text{C}_{27}\text{H}_{33}\text{ClFeSi}_3$ 534.0899) (1.9) [$\text{M}^+ - 2\text{CO}$].

5.7. (1-Methyl-3,4-diphenyl-2,5-bis(trimethylsilyl)-1-silacyclopentadienyl)- η^5 -cyclopentadienyl-dicarbonyl-iron (**16**)

1.06 g (2.48 mmol) $\text{K}[\text{Fe}(\text{CO})_2\text{Cp}]$ was dissolved in 10 mL tetrahydrofuran and cooled to $-40\text{ }^{\circ}\text{C}$. 0.53 g (2.48 mmol) **13** in 10 mL tetrahydrofuran was added dropwise at $-40\text{ }^{\circ}\text{C}$. The colour of the mixture became brown during the addition and the mixture was stirred for 4 h at $-40\text{ }^{\circ}\text{C}$. After that it was allowed to warm to room temperature and was stirred overnight. The solvent was removed under reduced pressure and 20 mL hexane was added to the residue. The resulting insoluble white salt was filtered out and the brown filtrate was concentrated under reduced pressure and crystallized at $-30\text{ }^{\circ}\text{C}$. The pure compound was obtained by recrystallized from hexane at $-30\text{ }^{\circ}\text{C}$ resulting in yellow cubic crystals. Yield: 1.14 g (90%) Anal. calcd. for $\text{C}_{30}\text{H}_{36}\text{Si}_3\text{FeO}_2$ (568.71): C, 63.25; H, 6.55. Found: C, 63.37; H, 6.18. ^1H NMR (CDCl_3): $\delta = 0.11$ (s, 18H, SiMe₃), 0.90 (s, 3H, CH₃), 4.26 (s, 5H, Cp), 6.65–7.14 (m, 10H, Ph). $^{13}\text{C}\{^1\text{H}\}$ NMR (CDCl_3): $\delta = 1.7$ (SiMe), 1.8 (SiMe₃), 85.1 (Cp), 126.2 (*p*Ph), 127.1, 127.2, 129.4, 130.0 (*o/m*Ph), 143.4 (C _{α}), 154.8 (*i*Ph), 163.3 (C _{β}), 215.8 (CO). $^{29}\text{Si}\{^1\text{H}\}$ NMR (CDCl_3): $\delta = 55.5$ (Si-ring), -9.7 (SiMe₃). IR (nujol, cm^{-1}) $\nu(\text{CO})$ 1999, 1948. HRMS (EI): *m/z* (%) 568.1355 (calc. for $\text{C}_{30}\text{H}_{36}\text{FeO}_2\text{Si}_3$ 568.1367) (2.5) [M^+], 512.1469 (calc. for $\text{C}_{28}\text{H}_{36}\text{FeSi}_3$ 512.1469) (62.3) [$\text{M}^+ - 2\text{CO}$], 391.1721 (calc. for $\text{C}_{23}\text{H}_{31}\text{Si}_3$ 391.1734) (100.0) [$\text{M}^+ - \text{Fe}(\text{CO})_2\text{Cp}$].

5.8. Reaction of **13**, **14** with $\text{K}[\text{W}(\text{CO})_3\text{Cp}]$ and **14** with $\text{K}[\text{Fe}(\text{CO})_2\text{Cp}]$

$\text{K}[\text{W}(\text{CO})_3\text{Cp}]$ or $\text{K}[\text{Fe}(\text{CO})_2\text{Cp}]$ was dissolved in THF and the solution was cooled to $-40\text{ }^{\circ}\text{C}$. Solution of **13** or **14** in THF was added dropwise to this solution at $-40\text{ }^{\circ}\text{C}$. After stirring for 3 h at $-40\text{ }^{\circ}\text{C}$ the mixture was allowed to warm to room temperature followed by further stirring for 10 h or refluxing for 10 h. The solvent was removed under reduced pressure and 10 mL hexane was added to the residue. The resulting insoluble salt was filtered out and the filtrate was condensed at reduced pressure and the light-coloured solid was identified in all three cases as starting materials (**13**, **14**) according to NMR spectroscopy.

5.9. UV irradiation reactions

A 200 mg (0.34 mmol) of **15** were dissolved in 10 mL hexane. After the solution was irradiated with UV lamp for 30 min. The colour of the mixture became darker during the irradiation. After that the solvent was removed under reduced pressure and the residue was dissolved in CDCl_3 and NMR measurements were carried out, but the products could not be identified.

B 250 mg (0.44 mmol) of **16** was dissolved in 10 mL hexane. After the solution was irradiated with UV lamp for 30 min. The colour of the mixture became darker during the irradiation in all cases. After that the solvent was removed under reduced pressure and the residue was dissolved in hexane, filtered, and the solution was concentrated. The resulted colourless crystals were identified as **18**. Yield: 25 mg (10%), m.p. $224\text{--}226\text{ }^{\circ}\text{C}$. Anal. calcd. for $\text{C}_{46}\text{H}_{62}\text{Si}_6$ (783.49): C, 70.52; H, 7.98. Found: C, 70.45; H, 8.46. ^1H NMR (CDCl_3): $\delta = -0.01$ (s, 18H, SiMe₃), 0.78 (s, 3H, CH₃), 6.80–7.15 (m, 10H, Ph). $^{13}\text{C}\{^1\text{H}\}$ NMR (CDCl_3): $\delta = -0.7$ (SiMe), 1.7 (SiMe₃), 126.1, 126.8, 129.1, 142.8, 147.9, 170.0. $^{29}\text{Si}\{^1\text{H}\}$ NMR (CDCl_3): $\delta = 5.8$ (Si-ring), -9.9 (SiMe₃). HRMS (EI): *m/z* (%) 782.3481 (calc. for $\text{C}_{46}\text{H}_{62}\text{Si}_6$ 782.3462) (13.5) [M^+], 767.3207 (calc. for $\text{C}_{45}\text{H}_{59}\text{Si}_6$ 767.3227) (5.1) [$\text{M}^+ - \text{Me}$], 391.1727 (calc. for $\text{C}_{23}\text{H}_{31}\text{Si}_1$ 391.1734) (89.3) [$1/2\text{ M}^+$].

5.10. Reactions of **14** or **15** with Me_3NO

0.54 mmol **14** or **15** dissolved in 3 mL THF was added dropwise to the THF solution of 40 mg (0.54 mmol) trimethylamine N-oxide at $-20\text{ }^{\circ}\text{C}$. The mixture was stirred for 30 min at $-20\text{ }^{\circ}\text{C}$. The reaction mixture did not show any change, therefore it was allowed to warm to room temperature and was stirred for another 30 min at that temperature. The insoluble solid was filtered out, the filtrate was concentrated under reduced pressure and crystallized at $-30\text{ }^{\circ}\text{C}$. The residue was identified as starting material based (**12** or **13**) on NMR measurements.

Acknowledgements

The authors thank the Institut für Anorganische Chemie, Karlsruher Institut für Technologie (KIT) for the measurements of NMR spectra, mass spectra and for elemental analysis. Financial support from the Hungarian Scientific Research Fund OTKA NN 113772, K-100801 and COST CM10302 (SIPS) is gratefully acknowledged.

Appendix A. Supplementary data

CCDC 1412535 (15), CCDC 1412536 (16) and CCDC 1412537 (18) contain the supplementary crystallographic data for this paper. These data can be obtained free of charge from The Cambridge Crystallographic Data Centre via www.ccdc.cam.ac.uk/data_

request/cif.

Appendix B. Supplementary data

Supplementary data related to this article can be found at <http://dx.doi.org/10.1016/j.jorganchem.2015.09.023>.

References

- [1] (a) T.J. Kealy, P.L. Pauson, *Nature* 168 (1951) 1039–1040;
(b) A. Togni, T. Hayashi (Eds.), *Ferrocenes. Homogenous Catalysis. Organic Synthesis. Materials Science*, VCH, Weinheim, 1995;
(c) A. Togni, R. Halterman (Eds.), *Metalloenes: Synthesis, Reactivity, Applications*, VCH, Weinheim, 1998;
(d) Issue dedicated to 50th anniversary of ferrocene synthesis, *J. Organomet. Chem.* 637–639 (2001) 1–8751;
(e) G. Wilkinson, M. Rosenblum, M.C. Whiting, R.B. Woodward, *J. Am. Chem. Soc.* 74 (1952) 2125–2126.
- [2] (a) M. Driess, D. Hu, H. Pritzkow, H. Schaufele, U. Zenneck, M. Regitz, W. Rösch, *J. Organomet. Chem.* 334 (1987) C35–C38;
(b) M.L. Sierra, N. Maigrot, C. Charrier, L. Ricard, F. Mathey, *Organometallics* 11 (1992) 459–462;
(c) A.J. Ashe III, J.W. Kampf, S.M. Al-Taweel, *Organometallics* 11 (1992) 1491–1496;
(d) A.J. Ashe III, J.W. Kampf, S. Pilotek, R. Rousseau, *Organometallics* 13 (1994) 4067–4071;
(e) A.J. Ashe III, S. Al-Ahmad, S. Pilotek, D.B. Puranik, C. Elschenbroich, A. Behrendt, *Organometallics* 14 (1995) 2689–2698;
(f) S.J. Black, M.D. Francis, C. Jones, *J. Chem. Soc. Dalton Trans.* (1997) 2183–2190;
(g) X. Sava, L. Ricard, F. Mathey, P. Le Floch, *Organometallics* 19 (2000) 4899–4903;
(h) E. Urnezius, C.J. Cramer, J.E. Ellis, W.W. Brennessel, P. v. R. Schleyer, *Science* 295 (2002) 832–834;
(i) S. Welsch, L.J. Gregoriades, M. Sierka, M. Zabel, A.V. Virovets, M. Scheer, *Angew. Chem. Int.* 46 (2007) 9323–9326;
(j) R.S.P. Turbervill, A.R. Jupp, P.S.B. McCullough, D. Ergöcmen, J.M. Goicoechea, *Organometallics* 32 (2013) 2234–2244;
(k) M. Fleischmann, S. Welsch, H. Krauss, M. Schmidt, M. Bodensteiner, E.V. Peresypkina, M. Sierka, C. Grcger, M. Scheer, *Chem. Eur. J.* 20 (2014) 3759–3768.
- [3] W.P. Freeman, T.D. Tilley, A.L. Rheingold, R.L. Ostrander, *Angew. Chem. Int.* 32 (1993) 1744–1745.
- [4] W.P. Freeman, J.M. Dysard, T.D. Tilley, A.L. Rheingold, *Organometallics* 21 (2002) 1734–1738.
- [5] W.P. Freeman, T.D. Tilley, *J. Am. Chem. Soc.* 116 (1994) 8428–8429.
- [6] H. Yasuda, Y.L. Vladimir, A. Sekiguchi, *J. Am. Chem. Soc.* 131 (2009) 9902–9903.
- [7] Y.L. Vladimir, R. Kato, A. Sekiguchi, A. Krapp, G. Frenking, *J. Am. Chem. Soc.* 129 (2007) 10340–10341.
- [8] (a) J.M. Dysard, T.D. Tilley, *J. Am. Chem. Soc.* 120 (1998) 8245–8246;
(b) J.M. Dysard, T.D. Tilley, *J. Am. Chem. Soc.* 122 (2000) 3097–3105.
- [9] M.D. Curtis, *J. Am. Chem. Soc.* 91 (1969) 6011–6018.
- [10] A. Marinetti-Mignani, R. West, *Organometallics* 6 (1987) 141–144.
- [11] E. Colomer, R.J.P. Corriu, M. Lheureux, *Organometallics* 8 (1989) 2343–2348.
- [12] C. Fekete, I. Kovács, L. Könczöl, Z. Benkő, L. Nyulászi, *Struct. Chem.* 25 (2014) 377–387.
- [13] C. Fekete, I. Kovács, L. Nyulászi, *Phosphorus, Sulfur, Silicon* 189 (2014) 1076–1083.
- [14] R.-Z. Jin, K. Tamao, *Organometallics* 16 (1997) 2230–2232.
- [15] S. Fortier, Y. Zhang, H.K. Sharma, K.H. Pannell, *Organometallics* 29 (2010) 1041–1044.
- [16] A.L. Spek, *Acta Cryst. D65* (2009) 148–155.
- [17] J. Braddock-Wilking, Y. Zhang, J.Y. Corey, N.P. Rath, *J. Organomet. Chem.* 693 (2008) 1233–1242.
- [18] C.G. Pitt, *J. Organomet. Chem.* 61 (1973) 49–70.
- [19] D.L. Lichtenberger, A. Rai-Chaudhuri, *J. Am. Chem. Soc.* 113 (1991) 2923–2930.
- [20] H. K-Pannell, G.J. Long, *J. Organomet. Chem.* 186 (1980) 85–90.
- [21] J.A. Beumont, M.S. Wrighton, *Organometallics* 5 (1986) 1421–1429.
- [22] L. Nyulászi, *Chem. Rev.* 101 (2001) 1229–1246.
- [23] (a) H. Sohn, R.R. Huddleston, D.R. Powell, R. West, *J. Am. Chem. Soc.* 121 (1999) 2935–2936;
(b) S. Yamaguchi, R.-Z. Jin, K. Tamao, *J. Am. Chem. Soc.* 121 (1999) 2937–2938;
(c) R. Pietschnig, R. West, D.R. Powell, *Organometallics* 19 (2000) 2724–2729;
(d) Y. Liu, T.C. Stringfellow, D. Ballweg, I.A. Guzei, R. West, *J. Am. Chem. Soc.* 124 (2002) 49–57;
(e) S.J. Toal, H. Sohn, L.N. Zakarov, W.S. Kassel, J.A. Golen, A.L. Rheingold, W.C. Troglor, *Organometallics* 24 (2005) 3081–3087.
- [24] S.L. Hinchley, H.E. Robertson, A. Parkin, D.W.H. Rankin, G. Tekautz, K. Hassler, *Dalton Trans.* 24 (2004) 759–766.
- [25] N. Wiberg, H. Schuster, A. Simon, K. Peters, *Angew. Chem. Int.* 25 (1986) 79–80.
- [26] D.J. Blumer, K.W. Barnett, T.L. Brown, *J. Organomet. Chem.* 173 (1979) 71–76.
- [27] A. Ariafard, E.S. Tabatabaie, B.F. Yates, *J. Phys. Chem. A* 113 (2009) 2982–2989.
- [28] (a) M.W. Schmidt, P.N. Truong, M.S. Gordon, *J. Am. Chem. Soc.* 109 (1987) 5217–5227;
(b) M.W. Schmidt, M.S. Gordon, *Inorg. Chem.* 25 (1986) 248–254;
(c) P.v.R. Schleyer, D. Kost, *J. Am. Chem. Soc.* 110 (1988) 2105–2109.
- [29] M.J. Bennett Jr., F.A. Cotton, A. Davison, J.W. Faller, S. Lippard, S.W. Morehouse, *J. Am. Chem. Soc.* 88 (1966) 4371–4376.
- [30] G.M. Sheldrick, *SHELX-2013 Program for Crystal Structure Solution and Refinement*, University of Göttingen, Germany, 2013.
- [31] C.F. Macrae, P.R. Edgington, P. McCabe, E. Pidcock, G.P. Shields, R. Taylor, M. Towler, J. van de Streek, *J. Appl. Cryst.* 39 (2006) 453–457.
- [32] M.J. Frisch, G.W. Trucks, H.B. Schlegel, G.E. Scuseria, M.A. Robb, J.R. Cheeseman, G. Scalmani, V. Barone, B. Mennucci, G.A. Petersson, H. Nakatsuji, M. Caricato, X. Li, H.P. Hratchian, A.F. Izmaylov, J. Bloino, G. Zheng, J.L. Sonnenberg, M. Hada, M. Ehara, K. Toyota, R. Fukuda, J. Hasegawa, M. Ishida, T. Nakajima, Y. Honda, O. Kitao, H. Nakai, T. Vreven, J.A. Montgomery, J.E. Peralta, F. Ogliaro, M. Bearpark, J.J. Heyd, E. Brothers, K.N. Kudin, V.N. Staroverov, T. Keith, R. Kobayashi, J. Normand, K. Raghavachari, A. Rendell, J.C. Burant, S.S. Iyengar, J. Tomasi, M. Cossi, N. Rega, J.M. Millam, M. Klene, J.E. Knox, J.B. Cross, V. Bakken, C. Adamo, J. Jaramillo, R. Gomperts, R.E. Stratmann, O. Yazyev, A.J. Austin, R. Cammi, C. Pomelli, J.W. Ochterski, R.L. Martin, K. Morokuma, V.G. Zakrzewski, G.A. Voth, P. Salvador, J.J. Dannenberg, S. Dapprich, A.D. Daniels, O. Farkas, J.B. Foresman, J.V. Ortiz, J. Cioslowski, D.J. Fox, *Gaussian 09, Revision B.01*, Gaussian, Inc., Wallingford, 2010.
- [33] A. Todd, T.K. Keith, *Gristmill Software*. 510 Overland Park AIMail 11.10.16, 2011. <http://aim.tkgristmill.com>.
- [34] G. Schaftenaar, J.H. Noordik, *J. Comput. Aided. Mol. Des.* 14 (2000) 123–134.